УДК 541.145 doi: 10.33609/2708-129X.89.12.2023.88-109

THE INFLUENCE OF THE PHASE COMPOSITION OF MIXED-PHASE MESOPOROUS TiO_2 ON ITS PHOTOCATALYTIC ACTIVITY IN THE REACTION OF HYDROGEN EVOLUTION FROM AN AQUEOUS-ETHANOL MIXTURE.

N. I. Ermokhina[1], V.V. Shvalagin [1], G. V. Korzhak[1], V. N. Grebennikov[1]*, N. I. Romanovska[1], A. V. Shulzshenko[1], M. M. Shcherbatyuk[2], D. O. Klymchuk[2], P. A. Manorik[1]

[1] Pisarzhevskii Institute of Physical Chemistry of the National Academy of Sciences of Ukraine, 31 Ave. Science, 03028 Kyiv, Ukraine
[2] Institute of Botany of the National Academy of Sciences of Ukraine, 2 Tereshchenkivska St., 01601 Kyiv, Ukraine
**e-mail: vng@ukr.net*

Two- and three-phase compositions of mesoporous nanocrystalline TiO_2 (meso-nc-TiO_2) were obtained from sol-gel reaction mixtures (ZGRM) using dibenzo-18-crown-6 (DB18C6) as a structure-directing agent and titanium tetrabutoxide (TBOT) as a source of titanium in the presence of HCl with (or without) subsequent hydrothermal treatment (HTT) and calcination at 500 °C.

It has been shown that the addition of a small amount of dodecyldimethylethylammonium bromide (DDMEABr) and/or lanthanum salts in ZGRM, as well as HTT, has a significant effect on the phase composition and texture of the samples. It was established that the use of HTT before calcination of samples significantly increases their photocatalytic activity (PhA) in the reaction of photocatalytic hydrogen release from an aqueous-ethanol mixture mainly due to changes in their phase composition.

The hydrothermally treated sample of the anatase (85%)/rutile (4%)/brookite (11%) phase composition shows the highest photocatalytic activity, which is 2.5 times higher than the corresponding characteristic for the commercial Evonik P25 photocatalyst. It is shown that the size of the specific surface area of the sample is not the dominant factor influencing the photocatalytic activity of the obtained mixed-phase meso-nc-TiO_2 samples in the process of hydrogen release from the aqueous-ethanol mixture.

Keywords: sol-gel synthesis, mesoporous TiO_2 anatase-rutile-brookite compositions, H_2 release.

INTRODUCTION. The need to ensure the sustainable development of post-industrial society, the rapid deepening of planetary energy and environmental problems require obtaining new materials for modern equipment and technologies. In particular, such materials include electrode materials for solar cells, photocatalysts for cleaning the environment (water and air) from various pollutants using sunlight energy, etc. [1, 2]. Today, in the field of semiconductor photocatalytic technology, materials based on TiO_2 occupy a leading position both in terms of demand and research intensity due to the unique properties of TiO_2 and, above all, non-toxicity, chemical stability and commercial availability [1–17].

One of the most advanced methods of obtaining TiO_2 and other mesoporous oxides today remains the sol-gel method, which involves the use of a template [10, 13, 14, 18]. Combining it with the widely used method of solvo(hydro)thermal treatment of an intermediate product allows controlling the processes of formation of unique TiO_2 materials with a given phase composition, morphology and texture at the nano-level [19, 20]. To achieve the full catalytic potential of the obtained TiO_2 materials, they usually require calcination at a temperature of about 500 °C [21, 22].

The efficiency of the TiO_2 photocatalyst depends on a number of factors, in particular the degree of crystallinity and crystallite size, phase composition, morphology of nanoparticles, textural characteristics, etc. [1, 2, 6, 7]. The main ways to increase the efficiency of TiO_2 photocatalysts are to expand their spectral range of light absorption into the visible region by doping with nonmetals, metals, sensitization with dyes, obtaining nanocomposites with nanoparticles, obtaining heterostructures with other semiconductors, etc. [1, 2, 7]. At the same time, for example, in the case of nanocomposites and heterostructures, an additional increase in the PhA of TiO_2 photocatalysts is achieved due to the suppression of the recombination of photogenerated charge carriers [1, 2, 7].

Among the three main crystalline forms of TiO_2 (anatase, rutile, and brookite), anatase usually has the highest photocatalytic activity (PhA) [23]. However, a number of experimental facts indicate that TiO_2 nanostructures in which several TiO_2 crystalline phases are combined [11, 12, 15, 24–28] show a higher PhA than the corresponding single-phase nanostructures. A classic example of such mixed-phase structures is Degussa P25 Evonik P25, which consists of anatase (75%) and rutile (25%), and which is used as a standard in studies of the photocatalytic activity of materials [29]. The results obtained in studies of two- and three-phase TiO_2 polymorphs sometimes lead to contradictory conclusions when comparing the photocatalytic activity of compositions of TiO_2 phases in various redox processes [2, 24–31]. At the same time, taking into account the fact that the preparation of heterostructures from several semiconductors, which differ in the band gap, is one of the effective ways to increase the PhA of photocatalysts [1, 2, 7], and that there are no fundamental differences between such heterostructures and mixed phases of TiO_2, which have different widths of the band gap, the search for conditions for the synthesis of such mixed-phase materials based on titanium dioxide, which can provide a controlled variation of the phase composition of the obtained materials, and, accordingly, their PhA, seems very promising.

Earlier [28] we proposed an approach to obtaining mixed-phase TiO_2 nanostructures (anatase/brookite) with increased PhA. However, due to the chemical features of the components of the sol-gel reaction mixture, this approach does not allow varying the phase composition of the obtained material within wide limits. It was also proposed to obtain mesoporous nanocrystalline TiO_2 (meso-nc-TiO_2) with a pure anatase structure by combining sol-gel synthesis with HTT of an intermediate product [32–36]. TiO_2 samples calcined at 500°C after HTT at 175°C had a significantly more developed porous structure compared to untreated hydrothermally treated samples. It was shown that the introduction of small additions of cationic surfactant (DDMEABr) and (or) lanthanum salt into the reaction mixture has a significant effect on the degree of crystallization, morphology and texture of meso-nc-TiO_2 (anatase) samples and their photocatalytic activity. Practically all the obtained samples were highly efficient photocatalysts for the processes of water reduction, gas-phase oxidation of alcohol and benzene [34–38]. This approach can be used to vary the phase composition of mixed-phase TiO_2 materials over a wide range.

This paper considers the influence of varying the synthesis conditions of meso-nc-TiO_2 samples on their phase composition, as well as the influence of the phase composition of meso-nc-TiO_2 samples both in the form of pure anatase and various mixed-phase compositions (anatase-brookite-rutile), which consist of two or three phases, on their photocatalytic properties in the reaction of the release of molecular hydrogen from a aqueous-ethanol mixture.

EXPERIMENT AND RESULTS DISCUSSION. The work used titanium tetrabutoxide (IV), dodecyldimethylethylammonium bromide, dibenzo-18-crown-6 ("Fluka"), HCl, n-butanol, LaCl3•7H_2O, CuCl2, NaCl, ethanol (96%), TiO_2 Evonik P25.

Samples of meso-nc-TiO_2 with different contents of rutile anatase and brookite were obtained using the modified sol-gel method similarly [32, 33]. Hydrolysis of titanium tetrabutoxide was carried out in butanol in the presence of HCl using as a structure-directing agent the complex of sodium with dibenzo-18-crown-6 [Na(DB18C6)]Cl in the presence (or without) of small additions of the surfactant DDMEABr and a lanthanum salt. The calculated amounts of reagents were successively dissolved in butanol. TBOT was added dropwise with vigorous stirring. The reaction mixture was left under a glass cap in air at room temperature (without stirring) until the formation of the gel stopped. The obtained product was subjected to HTT at 175 °C for 24 hours followed by annealing at 500 °C in air for 4 hours.

The meso-nc-TiO_2 samples obtained under different conditions are denoted as Ti n and Ti nH, where n is the sample number and H is the hydrothermal treatment. The molar composition of the reaction mixture, which was used for the synthesis of meso-nc-TiO_2 samples, is given in Table 1.

The X-ray diffraction (XRD) patterns of the samples was performed on a DRON-3M (CuKα) diffractometer. The average size of TiO_2 crystallites was calculated from the width of the diffraction peak of anatase (101) at $2\theta = 25.4^o$ according to the well-known Scherrer formula.

Table 1.

Synthesis conditions of meso-nc-TiO_2 samples ([TBOT]:[Na(DB18C6)]Cl = 1.0:0.02).

Sampler	Additive		BuOH	H_2O	HCl
	Surfactant**	La^{3+}			
Ti1	-	-	78	3	0,4
Ti1H	-	-	78	3	0,4
Ti2	0,02	-	78	3	0,4
Ti2H	0,02	-	78	3	0,4
Ti3	-	0,01	78	3	0,4
Ti3 H	-	0,01	78	3	0,4
Ti4	0,02	0,01	117	3	0,4
Ti4H	0,02	0,01	117	3	0,4
Ti5	0,02	0,01	78	3	0,4
Ti5H	0,02	0,01	78	3	0,4
Ti6 H	0,02	0,01	57	3	0,4
Ti7 H	0,02	0,01	26	7	0,7
Ti(MS1)*	-	-	78,0	-	-
Ti(MS1)H*	-	-	78,0	-	-
Ti(MS2)*	-	-	78,0	3,0	-
Ti(MS2)H*	-	-	78,0	3,0	-

* meso-nc-TiO_2 samples (microspheres) [36];
** surfactant – DDMEABr.

The morphology of the samples was studied by transmission (TEM) and scanning (SEM) electron microscopy using JEM 1230 and JSM-6060LA ("JEOL") microscopes, respectively. In some cases, the samples were pretreated for 5 min using an ultrasonic disperser UZDN-A (130 W).

N_2 adsorption/desorption isotherms were recorded at –196 °C on a gas-adsorption analyzer Autosorb-6 (Quantachrome). Before adsorption, the sample was pumped at 200 °C for 20 hours. The specific surface area (S_{BET}) and the average pore diameter (Dp) were determined by the BET та BJH methods, respectively. The pore size distribution was calculated from the desorption branch of the isotherm using the NLDFT method using a cylindrical pore model. The total amount of N_2 adsorbed at p/p0 = 0.997 was used to determine the total pore volume (Vtot).

The photocatalytic activity of the obtained meso-nc-TiO_2 samples was studied in a model reaction of photocatalytic hydrogen evolution from an aqueous-ethanol mixture. The reaction conditions were similar to those described in [39]. The TiO_2 samples were irradiated with UV light (λ = 310–390 nm) in a system containing a aqueous-ethanol mixture (4 vol. % H_2O) and $CuCl_2$ ($2 \cdot 10^{-4}$ mol/l). Commercial photocatalyst TiO_2 Evonik P25 was used as a comparison sample.

Samples of meso-nc-TiO_2 with different contents of anatase, rutile and brookite were obtained by a simple modification of our previously proposed approach [32, 33] - changing the conditions of TBOT hydrolysis, namely, by switching from a neutral to an acidic medium, using a well-known acid catalyst - hydrochloric acid [38, 39] (Table 1). The main concept of such optimization of the former synthetic approach is to combine the influence of factors: HTT, small additives of surfactant and (or) lanthanum salt, as well as the concentration of reagents in the reaction mixture in the presence of HCl on the phase composition of meso-nc-TiO_2 materials.

Previously [32-36] samples of thermally stable meso-nc-TiO_2 with a well-defined spherical morphology (microspheres of size from 0.6 to 3 μm with a pure anatase structure) were

obtained under conditions of neutral hydrolysis, characterized by different textures. Microspheres are formed by primary spherical particles (anatase crystallites about 10 nm in size), which are tightly packed into spherical mesoaggregates 30–70 nm in size (secondary particles), which form a mesopore system. Table 1 and 2 shows examples of synthesis conditions and textural characteristics of such TiO_2 microstructures.

Table 2.

Textural characteristics of meso-nc-TiO_2 samples, as well as their photocatalytic properties in the reaction of H_2 release from an aqueous-ethanol mixture.

Sample	S_{BET}, m^2/g	V_p, cm^3/g	D_{tot}, nm	Crystallite Size A, nm	Phase composition **			$H_2 \cdot 10^7$, mol/min
					A	R	B	
Ti1	39	0,14	14,5	9,8	29	39	32	2,5
Ti1H	61	0,29	18,9	10,4	34	14	52	3,0
Ti2	48	0,23	13,0	7,2	22	60	18	0,4
Ti2H	33	0,21	17,4	9,4	16	70	14	0,7
Ti3	83	0,21	9,4	7,1	55	21	24	1,8
Ti3H	64	0,30	17,3	8,2	43	28	29	2,9
Ti4	122	0,31	9,4	8,3	97	3	-	3,7
Ti4H	96	0,28	11,3	9,5	85	4	11	5,5
Ti5	98	0,18	7,0	7,4	88	-	12	2,0
Ti5H	132	0,46	13,9	7,0	100	-	-	3,0
Ti6H	90	0,44	17,3	9,1	90	-	10	2,8
Ti7H	100	0,30	12,3	10,2	25	45	30	4,7
Ti(MS1)*	61	0,14	9,0	10,5	100	-	-	3,8
Ti(MS1) H*	84	0,33	15,5	11,0	100	-	-	6,6
Ti(MS2)*	97	0,30	12,3	8,7	100	-	-	4,0
Ti(MS2) H*	116	0,50	17,3	10,0	100	-	-	5,0
P25	50	-	-	25	70	30	-	2,2

* [36]; **A – anatase, R – rutile, B – brookite.

ISSN 2708-129X. Укр. хім. журн., 2023

In Fig. 1 presents the diffraction patterns of meso-nc-TiO_2 (Ti1, Ti1H, and Ti4, Ti4H) samples obtained in an acidic environment in the presence of HC1. The phase content of the compositions in the samples was determined by the main diffraction peaks of anatase (JCPDS-PDF, No. 21–1272), rutile (JCPDS-PDF, No. 21–1276), and brookite (JCPDS-PDF, No. 29–1360), marked respectively as (101), (110) and (121) reflexes using known calculation methods. According to the XRD, pattern of Ti4 sample contain low-intensity narrow peaks at 32° and 45.5° (2θ), which can be attributed to NaCl occluded in the synthesis process [33]. The calculated average sizes of anatase crystallites in the samples range from 7.0 to 10.4 nm (Table 2). The most important samples are Ti1 (9.8 nm) and Ti1H (10.4 nm), obtained without additives of sulfactant or lanthanum salt.

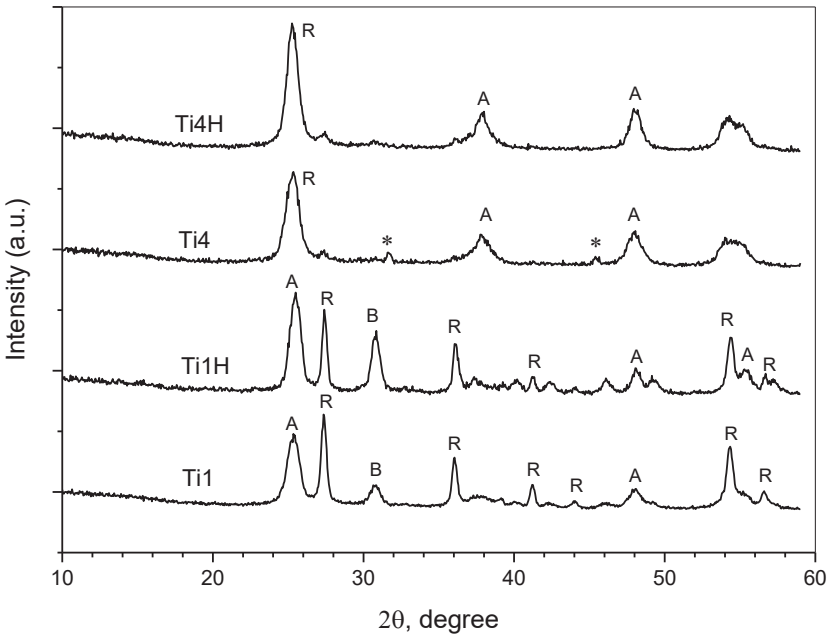

Fig. 1 XRD patterns of meso-nc-TiO_2: Ti1, Ti1H and Ti4, Ti4H samples, obtained in various synthetic conditions; A – anatase, R – rutile, B – brookit.

In Fig. 2 presents N_2 adsorption/desorption isotherms and pore size distribution for meso-nc-TiO_2 samples. All isotherms belong to type IV (according to the IUPAC classification) with H1 and H2 hysteresis loops located at values of relative pressure p/p_0 above 0.6, which indicates the formation of mesopores in the obtained samples.

Textural characteristics and phase composition of meso-nc-TiO_2 samples are shown in Table 2. All of them contain anatase phase, the proportion of which covers a wide range from 16 to 100%. At the same time, the content of rutile ranges from 0 to 70%, and brookite from 0 to 52%. The average size of anatase crystallites in the samples is about 10 nm. Most of the meso-nc-TiO_2 samples are three-phase compositions. In samples that contain two TiO_2

phases (anatase with rutile or brookite), the anatase phase predominates (88–97%) and one sample contains only anatase.

As can be seen from Fig. 1 and Table 2, the phase composition of the meso-nc-TiO_2 samples is affected by both the presence of DDMEABr surfactant additives, lanthanum salt, and the concentration of reagents in the reaction mixture during synthesis and the mode of heat treatment (use or absence of HTT before calcination) of the samples. Thus, the addition of DDMEABr leads to a decrease in the content of anatase and brookite and an increase in the content of rutile (sample Ti1), and the differences dramatically deepen in the case of HTT of these samples (sample Ti1H). It is the presence of the surfactant additive that makes it possible to obtain a Ti2H sample with the highest content of the rutile phase – 70%.

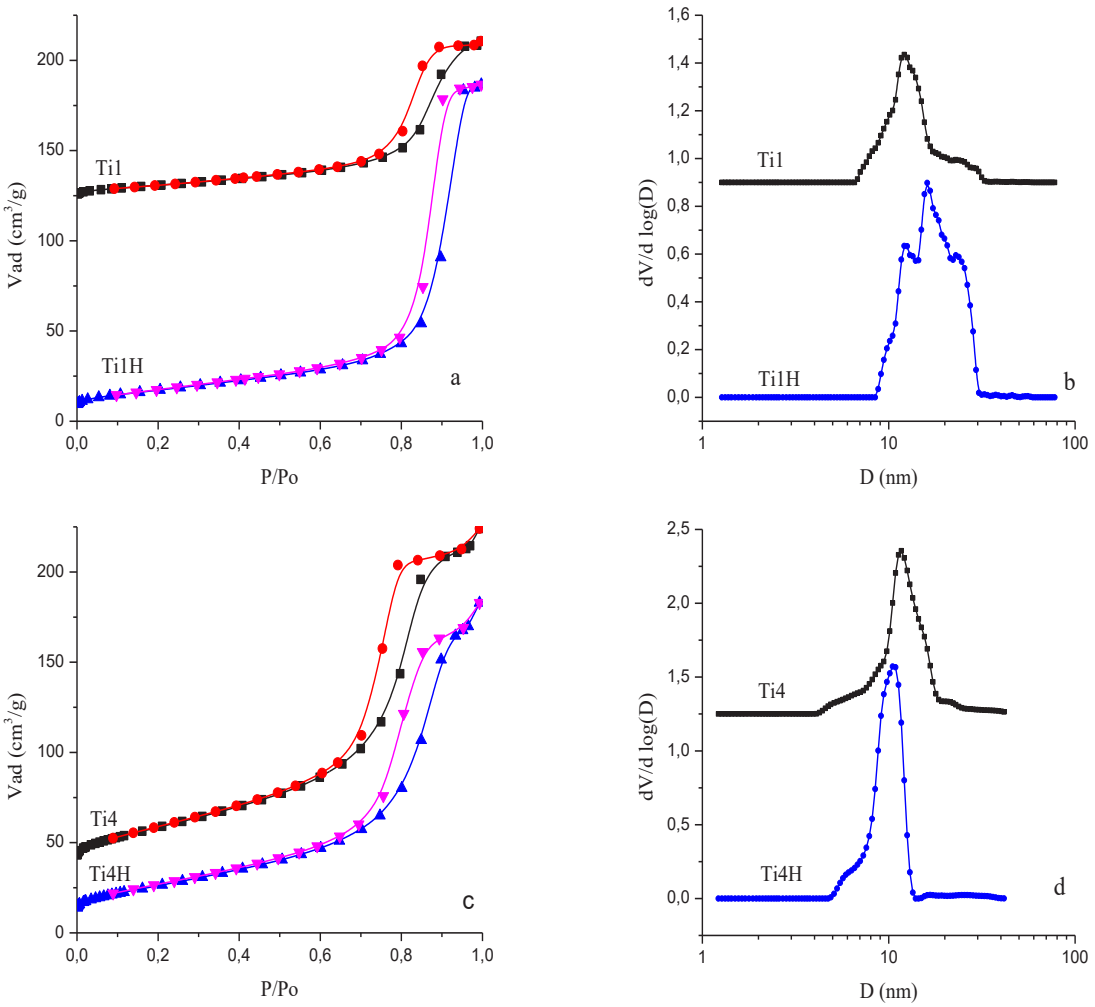

Fig. 2 N_2 adsorption/desorption isotherms and pore size distribution (obtained by the NLDFT method) of meso-nc-TiO_2 samples: Ti1 and Ti1H (a, b), Ti4 and Ti4H (c, d).

ISSN 2708-129X. Укр. хім. журн., 2023

The addition of lanthanum salt contributes to an increase in the content of anatase and a decrease in the content of brookite regardless of the use of HTT of the samples (samples Ti1, Ti1H and Ti3, Ti3H), while without the use of HTT the content of rutile decreases (samples Ti1 and Ti3), and when using HTT (samples Ti1H and Ti3H) increases. In the case of the samples obtained with the simultaneous presence of DDMEABr and lanthanum salts (Ti1, Ti1H and Ti5, Ti5H, T6H) in the ZGRM, a three-fold increase in the content of anatase is observed against the background of a sharp drop in the content of brookite and the complete disappearance of the rutile phase. The phase composition of the samples undergoes especially profound changes when using HTT (samples Ti1H and Ti5H), as a result of which the three-phase composition is transformed into a single-phase anatase (Fig. 1, Table 2).

Dilution of the original ZGRM in the presence of lanthanum salt additive (samples Ti3, Ti3H and Ti4, Ti4H) causes a two-fold increase in the amount of anatase with a simultaneous decrease in the content of brookite and rutile phases. So, for example, sample Ti3 consists of anatase (55%), rutile (21%) and brookite (24%), and the corresponding sample Ti4 consists of anatase (97%) and rutile (3%). Increasing the concentration of reagents in ZGRM containing DDMEABr additives and lanthanum salts (samples Ti5H, Ti6H, and Ti7H) makes it possible to obtain one-, two-, and three-phase compositions of TiO_2 (Fig. 1, Table 2). An increase in the concentration of H2O and HC1 in the ZGRM in the case of sample Ti7H significantly affects the phase composition of this sample in comparison with samples Ti5H and Ti6H. The mode of heat treatment obviously in all cases significantly affects the phase composition of meso-nc-TiO_2 (samples Ti1 and Ti1H, Ti2 and Ti2H, Ti3 and Ti3H, Ti4 and Ti4H, Ti5 and Ti5H). So, for example, sample Ti1, which was subjected only to calcination, is a composition of anatase (29%), rutile (39%) and brookite (32%), and sample Ti1H (which was previously subjected to HTT before annealing) contains anatase (34%), respectively), rutile (14%) and brookite (52%). It should be noted that among all the meso-nc-TiO_2 samples, the Ti1H sample (obtained without additives) contains the largest amount of brookite.

The presence of a surfactant additive in ZGRM (Table 2) leads to a slight increase in the value of $S_{BET.}$ in the case of calcined samples Ti1 (39 m^2/g) and Ti2 (48 m^2/g). At the same time, in the case of Ti1H (61 m^2/g) and Ti2H (33 m^2/g) samples, which were previously subjected to HTT, on the contrary, there is an almost two-fold decrease in the value of $S_{BET.}$ However, the surfactant practically does not affect the size of the diameter of the specified pores pairs of samples. The introduction of the lanthanum salt additive in the ZGRM provides a significant increase in S_{BET}. So, for example, the value of S_{BET} for sample Ti3 (89 m^2/g) increases by 2 times compared to Ti1 (39 m^2/g), which is probably due to an increase (doubled) in the content of the anatase phase, the nanoparticles of which form mesopores.

When diluting ZGRM by ~1.5 times, the specific surface area increases by the same amount (samples Ti3, Ti3H and Ti4, Ti4H), while the pore diameter decreases (samples Ti3H and Ti4H), which may be associated with the formation of these samples contain more anatase with smaller crystallites. This assumption is consistent with the results obtained for the Ti5H sample (Table 2). This sample, which contains the smallest crystallites among the

studied samples and consists of 100% anatase, has the highest value of S_{BET} (132 m^2/g) and volume V_{por} (0.46 cm^3/g) (Table 2). It should be noted that this sample, like Ti5H, was obtained with the simultaneous introduction of surfactant additives and La^{3+} ions into the ZGRM, which leads to a drastic increase in $S_{p.}$ of meso-nc-TiO_2 samples compared to the samples obtained only in the presence of surfactant additives (Ti2 and Ti2H samples) or La^{3+} ions (Ti3 and Ti3H samples). The reason for this may be the dominance of the anatase phase in Ti5 and Ti5H, the crystallite sizes of which are the smallest among the studied samples (Table 2). This assumption is consistent with the results of a comparison of the textural characteristics of the Ti5H sample with the T6H sample, which was obtained using higher concentrations of reagents in ZGRM than for Ti5H (Table 1, Table 2). Thus, an increase in the concentration of initial reagents in the ZGRM leads to a one-and-a-half-fold decrease in $S_{BET.}$, a significant increase in Dp (~25%) with an unchanged pore volume and a significant increase in the average size of anatase crystallites (from 7.0 to 9.1 nm).

A comparison of the textural characteristics of samples Ti2 and Ti2H (obtained in the presence of a surfactant additive), Ti3 and Ti3H, Ti4 and Ti4H (obtained in the presence of a lanthanum salt additive) shows that the previous HTT calcination leads to a decrease in S_{BET} (~20–30%) and a significant increase in Dp (~20-80%). A significant change in the pore volume (an increase of almost 1.5 times) occurs only in the case of the Ti3H sample. In the case of Ti5 and Ti5H samples (obtained with the simultaneous presence of La^{3+} ions and surfactant additives), on the contrary, the Ti5H sample, which underwent hydrothermal treatment before calcination, compared to the simply calcined Ti5 sample, shows an increase in S_{BET} (~35%) with a simultaneous increase of ~ 2.5 times V_{tot} and 2 times Dp, probably due to an increase in the content of anatase and a decrease in the size of crystallites.

In Fig. 3(b, d, e, h) shows examples of SEM images of meso-nc-TiO_2 microphase samples, which were obtained in the presence of HCl. As can be seen, there are no microspheres in samples Ti1 and Ti1H, Ti2 and Ti2H obtained with and without HTT. Obviously, hydrochloric acid prevents the formation of microspheres. All meso-nc-TiO_2 samples obtained in an acidic environment are amorphous aggregates of various sizes from 100 to 500 nm. During ultrasonic treatment of samples, these aggregates disintegrate into uniform nanosized secondary particles (40–100 nm) of spherical or spheroidal shape.

According to the results of TEM data (Fig. 3 (a, c, d, g) and Fig. 4(a - g)), all samples of meso-nc-TiO_2, with the exception of sample T7H (Fig. 4g), have homogeneous, spherical forms of primary particles (anatase phase). The sizes of anatase crystallites in the samples slightly exceed the corresponding values calculated according to Scherrer's formula (Table 2). Samples Ti1, Ti1H (Fig. 3(a, c)) and samples Ti2, Ti2H, Ti3, Ti3H (Fig. 4(a – d)), in which the percentage content of rutile and brookite phases is the highest, demonstrate the presence of crystallites in the form of various according to the size of plates having the shape of hexagons and quadrilaterals. Samples Ti1 and Ti1H contain the largest number of such particles, and the number of hexagons dominates (Fig. 3(a, c)). For samples Ti1 and Ti1H, the average sizes of hexagons are 80x30 nm, 110x50 nm, and 85x35 nm, 110x40 nm, and the average sizes of

quadrilaterals are 70x40 nm, 50x50 nm, and 80x60. In the Ti2 and Ti2H samples (Fig. 4(a, b)), on the contrary, square-shaped particles with an average size of 50x40 nm and 65x45 nm dominate, and the average size of hexagons is 100x45 nm and 90x50 nm. Ti3 and Ti3H samples (Fig. 4(c, d)) are significantly inferior in the number and size of hexagons (average size 75x30 nm and 80x25 nm), and tetragons (average size 60x35 nm) are present in small quantities only in the Ti3H sample. Samples Ti4 and Ti4H (Fig. 3(d, g)) have the smallest hexagons (50x20 nm and 65x30 nm). Samples Ti5, Ti5H, and T6H, which do not contain the rutile phase (Fig. 4(d - g)), consist only of spherical particles. The Ti7H sample (Fig. 4h) with a close content of three phases (Table 2) differs from other samples by the indistinct shapes of distorted particles, both spherical and polygonal in shape.

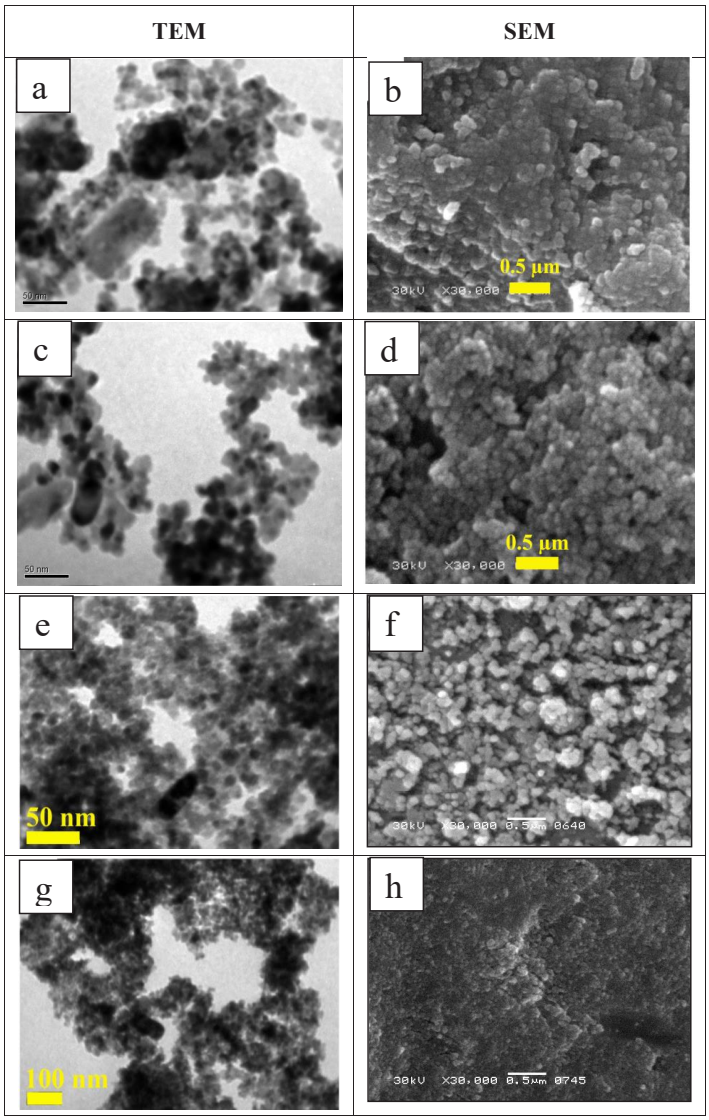

Fig. 3 TEM and SEM images of meso-nc-TiO_2 samples: Ti1 (a, b), Ti1H (c, d – after ultrasonic treatment), Ti4 (e, f), Ti4H (g, h – after ultrasonic treatment).

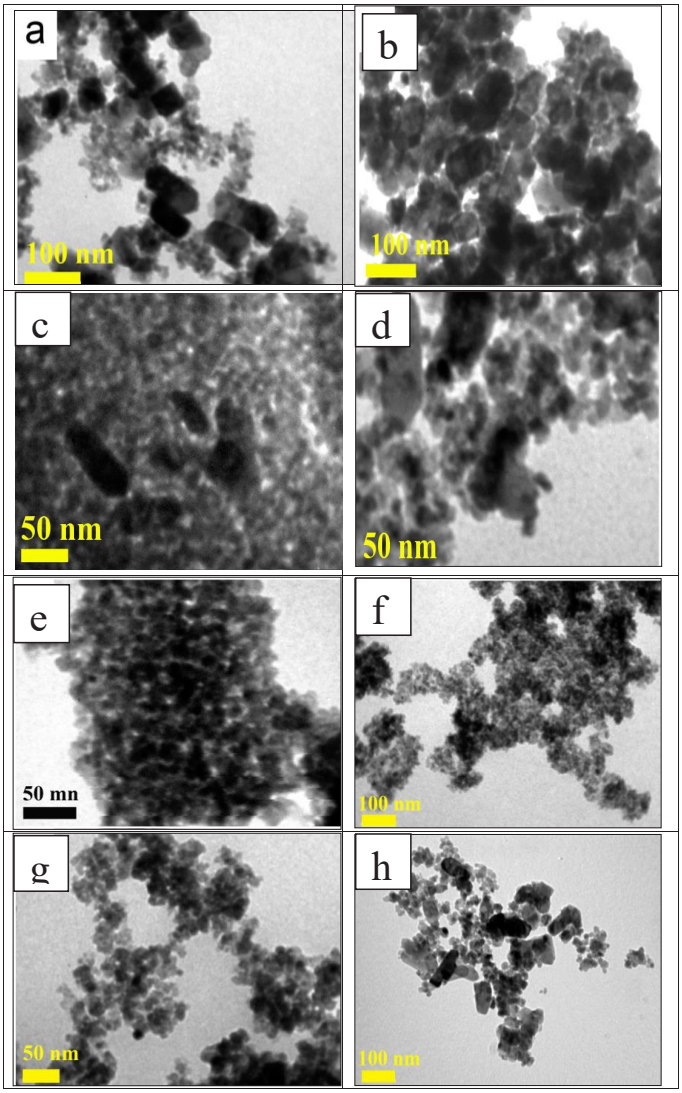

Fig. 4 TEM images of meso-nc-TiO_2 samples: Ti2 (a), Ti2H (b), Ti3 (c), Ti3H (d), Ti5 (e), Ti5H (f), Ti6H (g), Ti7H (h).

Thus, within the framework of one approach to sol-gel synthesis, a number of meso-nc-TiO_2 samples with different phase composition (anatase - rutile - brookite) were obtained in the presence of HCl in ZGRM. It is shown that small additions of surfactant and (or) lanthanum salts, HTT, as well as the concentration of reagents in the ZGRM affect the phase composition and texture of meso-nc-TiO_2 materials. This allows for a reliable comparative analysis of the obtained data on the photocatalytic activity of TiO_2 samples and to optimize the process of forming new photocatalysts with high activity.

The photocatalytic activity of meso-nc-TiO_2 samples of different phase composition (anatase - rutile - brookite) was studied in the model reaction of photocatalytic release of H_2 from an aqueous-ethanol mixture.

Earlier [42], we showed that samples of mesoporous TiO_2 (anatase) modified with Ni,

Ag, and Cu nanoparticles exhibit photocatalytic activity in the process of releasing H_2 from aqueous-ethanol mixtures. In these systems, photochemically deposited metal nanoparticles are co-catalysts that accept photogenerated electrons in the TiO_2 conduction zone and accelerate their transfer to the H_2O molecule. It was established [42] that copper nanoparticles are the most active co-catalyst. At the same time, the holes in the TiO_2 valence band are filled with the help of electron transfer from ethanol molecules. Under similar conditions, upon irradiation of the obtained meso-nc-TiO_2 samples with different phase composition, a rapid photodeposition process of copper nanoparticles occurs, which is visually recorded as a change in the color of the TiO_2 sample from white to dark brown. During the entire measurement period, the rate of H_2 release remains unchanged.

In Fig. 5a, as an example, kinetic dependences for samples Ti1H and Ti4H are given. At the same time, the commercial photocatalyst Evonik P25 shows much lower photocatalytic activity. As can be seen from Table 2, the rate of H_2 release in the presence of Evonik P25 is almost 1.5 and 2.5 times lower than the indicators of the above samples, respectively. The photocatalytic activity of Evonik P25, which consists of a mixture of nanocrystalline phases of anatase (~70%) and rutile (~30%) and has S_{BET} = 50 m^2/g and a particle size of 20-25 nm, is associated [31] with the possibility of spatial separation of photogenerated different charge carriers between anatase and rutile nanocrystals due to a small difference in the value of the conduction band potential of these TiO_2 phases.

Histograms and kinetic dependences presented in Fig. 5(a, b) show that most of the meso-nc-TiO_2 samples (Table 2) are significantly more active than Evonik P25 photocatalysts in the reaction of releasing H_2 from a aqueous-ethanol mixture Ti1, Ti3 and Ti5 are close in activity to sample P25, and Ti2H and Ti2 samples are significantly inferior by 3 and 5 times, respectively. The first two places in terms of photocatalytic activity are occupied by hydrothermally treated samples Ti4H and Ti7H. The highest activity in the case of samples Ti4H (1st place) and Ti4 (3rd place) can obviously be explained by the synergistic effect of anatase and rutile phases [12, 15], which is due to the combination of these phases in the mixed-phase compositions of Ti4H samples (anatase (85%) – rutile (4%) – brookite (11%)) and Ti4 (anatase (97%) – rutile (3%)). Moreover, even 2% of rutile in the composition of anatase – rutile causes an increase in the photocatalytic activity of such a photocatalyst [44]. A significant increase in the photocatalytic activity of anatase compositions with a small amount of rutile can be associated, as in the case of Evonik P25, with a different position of energy levels in anatase and rutile [12, 15, 31], which leads to a spatial separation of photogenerated charges between the components of the composition and accordingly, a decrease in electron-hole recombination. In the case of sample T7H (2nd place), high activity may be a consequence of the influence of the concentration conditions of the reagents used in the synthesis of this sample. The effect of HTT on increasing the photocatalytic activity of Ti1H-Ti5H samples (compared to Ti1-Ti5) is possibly a consequence of an increase in the size of the pore diameter in the treated samples. All samples, which are obtained in the presence of La^{3+} ion additives, are ahead of sample P25 in terms of activity. The only exception is sample Ti1 (close in activity to P25). This may be

related to the large value of the diameter of the pores of the sample Ti1 (14.5 nm). It is interesting to note the fact that the specific surface area of the studied meso-nc-TiO_2 samples and their phase composition are not key factors affecting their photocatalytic activity. For example, samples Ti4 and Ti5H have the maximum content of the anatase phase (97% and 100%, respectively) and the maximum value of S_{BET} (122 m^2/g and 132 m^2/g), and in the range of activity they occupy only 3 and 5 places, respectively.

Mixed-phase Ti1 and Ti1H samples consisting of anatase, rutile, brookite (Table 2) are significantly inferior in terms of activity obtained earlier [38] to samples of microspheres (anatase) Ti(MS1), Ti(MS2) and Ti(MS1)H, Ti(MS2)H, probably due to the fact that the special morphology of the microspheres provides much more efficient absorption of light quanta. The Ti(MS2)H sample outperforms both the Ti5H sample consisting of 100% anatase and all mixed-phase meso-nc-TiO_2 samples obtained in the presence of HCl in terms of photocatalytic activity (Table 2).

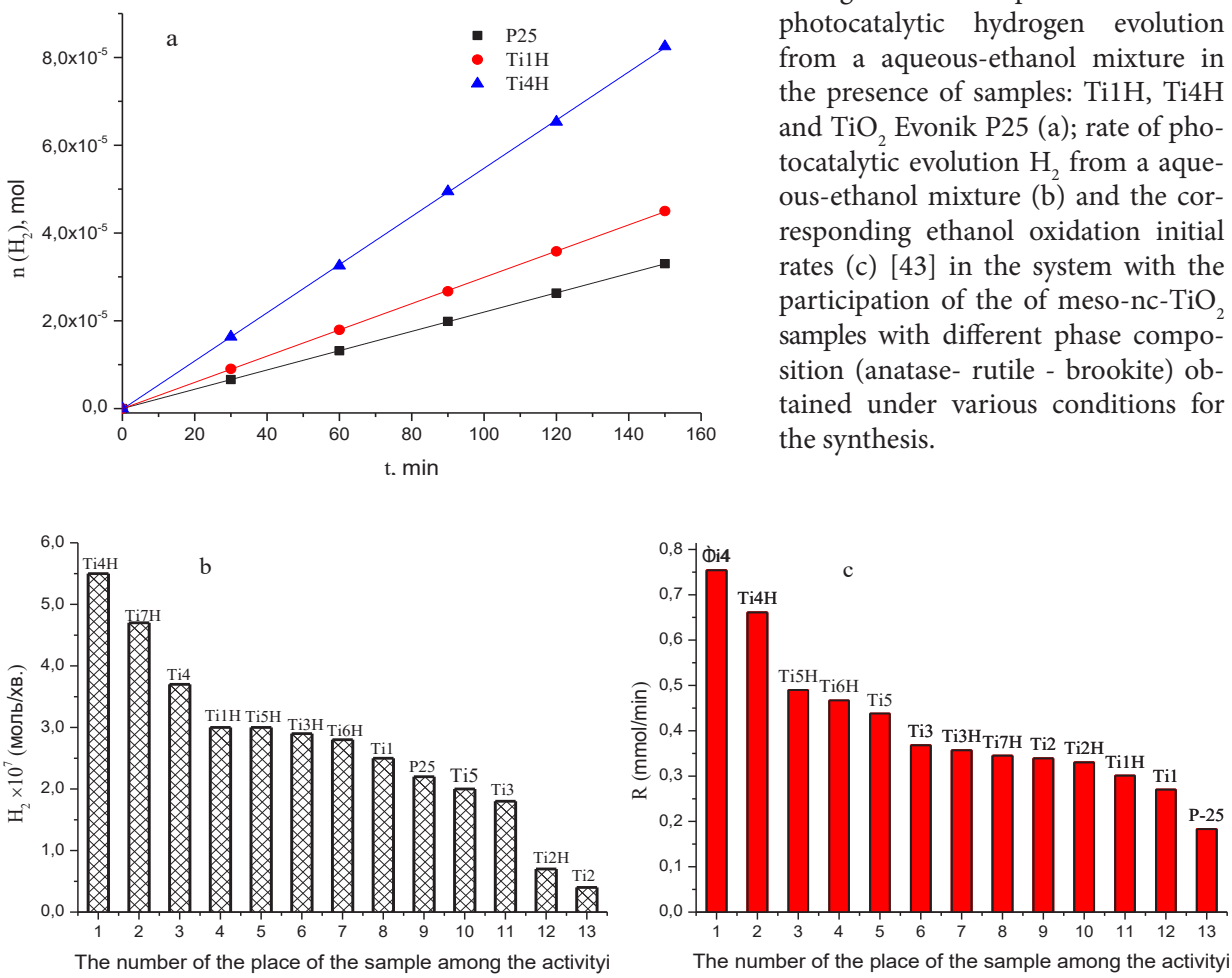

Fig. 5 Kinetic dependencies of the photocatalytic hydrogen evolution from a aqueous-ethanol mixture in the presence of samples: Ti1H, Ti4H and TiO_2 Evonik P25 (a); rate of photocatalytic evolution H_2 from a aqueous-ethanol mixture (b) and the corresponding ethanol oxidation initial rates (c) [43] in the system with the participation of the of meso-nc-TiO_2 samples with different phase composition (anatase- rutile - brookite) obtained under various conditions for the synthesis.

ISSN 2708-129X. Укр. хім. журн., 2023

The results of a comparison of histograms for the processes of H_2 release from an aqueous-ethanol mixture (Fig. 5b) and gas-phase oxidation of ethanol [43] (Fig. 5c) in the presence of mixed-phase meso-nc-TiO_2 samples are interesting. According to the histograms, in the process of ethanol oxidation, the most active samples Ti4, Ti4H, and Ti5H occupy 1, 2, and 3 places, and in the series of activity for the process of H_2 release, these samples occupy 3, 1, and 5 places, respectively. A similar picture is observed when comparing the histograms of these processes using meso-nc-TiO_2 (anatase) samples with the morphology of microspheres and nanopowders containing La^{3+} as photocatalysts [36-38].

According to the results shown in Table 2, the PhA of all three-phase samples that underwent preliminary HTT before calcination and differ significantly both in terms of textural characteristics and crystallite sizes is higher than that of Evonik P25, with the exception of the sample. Based on this, it can be assumed that all three phases (anatase, brookite and rutile) are responsible for the manifestation of photocatalytic activity. This assumption is especially clearly confirmed when comparing Ti4H and Ti5 samples, which are characterized by almost identical specific surface values (respectively 96 and 98 g/m^2) and have a close phase composition A/R/B (respectively 85/4/11 and 88/- /12). Here, the PhA of the Ti4H sample, which additionally contains 4% brookite, is 2.5 times higher than the PhA of the two-phase Ti5 sample, which does not contain brookite. This is probably due to the synergistic effect of three TiO_2 phases, the energy of the valence band and the conduction band of which are different, which contributes to the effective spatial separation of photogenerated charge carriers and, as a result, to the growth of the photocatalytic activity of mixed-phase samples. However, as can be seen from the results for Ti7H (Table 2), a significant increase in the content of the rutile and brookite phases and a decrease in the content of the anatase phase in the three-phase sample in comparison with, for example, the Ti4H sample leads to a decrease in the rate from 5.5 to 4.7 $H_2 \cdot 10^7$ mol/min, probably due to a decrease in the content of the anatase phase, which is the main source of photogenerated charge carriers. As can be seen from the results shown in Table 2, the three-phase samples are more efficient photocatalysts than the two-phase samples.

CONCLUSIONS. It was established that the variation of the synthesis conditions, namely the introduction of a small amount of dodecyldimethylethylammonium bromide (DDMEABr) and/or lanthanum salt into ZGRM, containing dibenzo-18-crown-6 (DB18C6) as a structure-directing agent and titanium tetrabutoxide (HTT) as a source of titanium. Decreasing or increasing the concentrations of the main reagents in the ZGRM, using HTT before calcining the samples has a significant effect on the phase composition and texture of the samples when standard heat treatment conditions are used (HTT at 175°C for 24 hours and annealing in air at 500 °C for 4 hours). This makes it possible to vary within fairly wide limits both the qualitative and quantitative composition of mixed-phase samples, their textural characteristics and photocatalytic activity.

It is shown that the use of HTT before calcination of samples significantly increases their photocatalytic activity in the reaction of photocatalytic release of hydrogen from an aqueous-ethanol mixture due to changes in their phase composition. In general, the obtained

three-phase meso-nc-TiO_2 samples are more effective photocatalysts than the two-phase samples. The PhA of all three-phase samples that underwent preliminary HTT before calcination and differ significantly both in terms of textural characteristics and crystallite sizes is higher than that of Evonik P25**.** Probably, all three phases (anatase, brookite and rutile) are responsible for the final value of photocatalytic activity due to the manifestation of the synergistic effect of three TiO_2 phases, the energy of the valence band and conduction band of which are different, which contributes to the effective spatial separation of photogenerated charge carriers and, as a result, the growth of photocatalytic activity mixed-phase samples. However, a significant increase in the content of the rutile and brookite phases and, accordingly, a decrease in the content of the anatase phase in the three-phase sample leads to a decrease in PhA, probably due to a decrease in the content of the anatase phase, which is the main source of photogenerated charge carriers.

The three-phase anatase (85%) rutile (4%) – brookite (11%) sample shows the highest photocatalytic activity among the studied samples, the PhA of which in the reaction of photocatalytic release of hydrogen from a aqueous-ethanol mixture exceeds the activity of the Evonik P25 sample by 2.5 times.

It was established that the use of HTT before calcination of the samples significantly increases their photocatalytic activity in the reaction of photocatalytic release of hydrogen from the aqueous-ethanol mixture mainly due to changes in their phase composition. At the same time, it is shown that the size of the specific surface of the sample is not the dominant factor affecting the photocatalytic activity of the obtained mixed-phase meso-nc-TiO_2 samples.

ACKNOWLEDGEMENT. The work was carried out within the framework of the state budget topic: "Composites based on doped TiO_2 nanostructures and coordination polymers: synthesis, phase composition, morphology and functional properties (state registration number: 0120U102376

ВПЛИВ ФАЗОВОГО СКЛАДУ ЗМІШАНОФАЗОВОГО МЕЗОПОРИСТОГО TiO_2 НА ЙОГО ФОТОКАТАЛІТИЧНУ АКТИВНІСТЬ У РЕАКЦІЇ ВИДІЛЕННЯ ВОДНЮ З ВОДНО-ЕТАНОЛЬНОЇ СУМІШІ

Н. І. Єрмохіна[1], В. В. Швалагін[1], Г. В. Коржак[1], В. М. Гребенніков[1]*, Н. І. Романовська[1], О. В. Шульженко[1], М. М. Щербатюк[2], Д. О. Климчук[2], П. А. Манорик[1]

[1]Інститут фізичної хімії ім. Л. В. Писаржевського НАН України;
просп. Науки, 31, Київ 03028, Україна
[2]Інститут ботаніки ім. М. Г. Холодного НАН України;
вул. Терещенківська, 2, Київ 01601, Україна
**e-mail:_vng@ukr.net*

Дво- і трифазові композиції мезопористого нанокристалічного TiO_2 (meso-nc-TiO_2) було отримано із золь-гель-реакційних сумішей (ЗГРС) із використанням дибензо-18-краун-6 (DB18C6) як структуроспрямовуючого агента і тетрабутоксиду титану (ТВОТ) як джерела титану за присутності HCl із (або без) подальшим гідротермальним обробленням (ГТО) і

прожарюванням за 500 °С. Показано, що добавляння невеликої кількості додецилдиметилетиламонію броміду (DDMEABr) та/або солі лантану в ЗГРС, а також ГТО справляють істотний вплив на фазовий склад та текстуру зразків. Встановлено, що використання ГТО перед кальцинуванням зразків суттєво підвищує їхню фотокаталітичну активність (ФА) в реакції фотокаталітичного виділення водню з водно-етанольної суміші головним чином завдяки змінам їхнього фазового складу. Найбільшу фотокаталітичну активність виявляє гідротермально оброблений зразок фазового складу анатаз (85%)/рутил (4%)/ брукіт (11%), яка у 2,5 рази перевищує відповідну характеристику для комерційного фотокаталізатора Evonik P25. Показано, що величина питомої поверхні зразка не є домінуючим фактором впливу на фотокаталітичну активність одержаних змішано-фазових зразків meso-nc-TiO_2 в процесі виділення водню з водно-етанольної суміші.

Ключові слова: золь-гель-синтез, мезопористий TiO_2 анатаз-рутил-брукіт-композиції, виділення H_2.

ЛІТЕРАТУРА

1. *Крюков А. І., Строюк А. Л., Кучмій С. Я., Походенко В. Д.* Нанофотокаталіз. Київ: Академперіодіка. 2013. 618 с.
2. *Schneider J., Bahnemann D., Ye J., Puma, G. Li., Dionysiou D. D.* Photocatalysis: fundamentals and perspectives // Royal Society of Chemistry. Cambridge. 2016. https://doi.org/10.1039/9781782622338
3. *Wang Y., Sun C., Zhao X., Cui B., Zeng Z., Wang A., Liu G., Cui H.* The application of nano-TiO_2 photo semiconductors in agriculture // Nanoscale Research Letters. 2016. 11. 1. P. 529. http://dx.doi.org/10.1186/s11671-016-1721-1
4. *Kumar N., Chauhan N.S., Mittal A., Sharma S.* TiO_2 and its composites as promising biomaterials: a review // BioMetals. 2018. 31. 2. P. 147–159. https://doi.org/10.1007/s10534-018-0078-6
5. *Noman M. T., Ashraf M. A., Ali A.* Synthesis and applications of nano-TiO_2: a review // Environmental Science and Pollution Research. 2019. 26. 4. P. 3262–3291. https://doi.org/10.1007/s11356-018-3884-z
6. *Humayun M., Raziq F., Khan A., Luo W.* Modification strategies of TiO_2 for potential applications in photocatalysis: a critical review // Green Chemistry Letters and Reviews. 2018. 11. 2. P. 86–102. https://doi.org/10.1080/17518253.2018.1440324
7. *Paul K. K., Giri P. K.* Shape tailored TiO_2 nanostructures and their hybrids for advanced energy and environmental applications: a review // Journal of Nanoscience and Nanotechnology. 2018. 19. 1. P. 307–331. https://doi.org/10.1166/jnn.2019.15778
8. *Dionysiou D. D., Puma G. Li., Ye J., Schneider J., Bahnemann D.* Photocatalysis: Applications. // Royal Society of Chemistry. Cambridge. 2016. P. 394. https://doi.org/10.1039/9781782627104
9. *Anpo M., Kamat P. V.* Environmentally benign photocatalysts // Springer. New York. 2010. https://doi.org/10.1007/978-0-387-48444-0
10. *Laura Cano-Casanova, Ana Amorós-Pérez, Maria Angeles Lillo-Ródenas and María del Carmen Román-Martínez.* Effect of the preparation method (sol–gel or hydrothermal) and conditions on the TiO_2 properties and activity for propane oxidation // Materials (Basel). 2018. 11. 11. P. 2227. https://doi.org/10.3390/ma11112227
11. *Verma R, Gangwar J, Srivastava A.K.* Multiphase TiO_2 nanostructures: a review of

efficient synthesis, growth mechanism, probing capabilities, and applications in bio-safety and health. // RSC Advances. 2017. **7**. 44199–44224.
https://doi.org/10.1039/C7RA06925A

12. *Bagheri S, Julkapli NM.* Mixed-phase TiO_2 photocatalysis: correlation between phase composition and photodecomposition of water pollutants // Reviews Inorganic Chemistry. 2017. 37. 1. 11–28.
https://doi.org/10.1515/revic-2016-0001
13. *Kumar A.* Different methods used for the synthesis of TiO_2 based nanomaterials: a review // American Journal of Nano Research and Application. 2018. 6. 1. P. 1.
https://doi.org/10.11648/j.nano.20180601.11
14. *Shayegan Z., Lee C-S., Haghighat F.* TiO_2 photocatalyst for removal of volatile organic compounds in gas phase: a review // Chemical Engineering Journal. 2018. 334. P. 2408–2439.
https://doi.org/10.1016/j.cej.2017.09.153
15. *Paul K.K, Giri P.K.* Shape tailored TiO_2 nanostructures and their hybrids for advanced energy and environmental applications: a review // Journal Nanoscience Nanotechnology. 2018. 19. 1. 307–331.
https://doi.org/10.1166/jnn.2019.15778
16. *Jiang, Z., Xu, X., Ma, Y. et al.* Filling metal–organic framework mesopores with TiO_2 for CO_2 photoreduction // Nature. 2020. 586. P. 549–554.
https://doi.org/10.1038/s41586-020-2738-2
17. *Jing Ma, Yang Tang, Gui Lu, Yu Wang, Wenke Niu, Dong Fu, Kai Zhang, Detlef W. Bahnemann, and Jia Hong Pan.* Incorporating Mesoporous Anatase TiO_2 Spheres to Conductive Carbon Black Filled PVDF Membrane for Self-Cleaning Photo (electro) catalytic Filtration // Journal of Physical Chemistry. C. 2023. 127. 17. 7998–8005.
https://doi.org/10.1021/acs.jpcc.3c01346
18. *Yang X., Konishi H., Xu H., Wu M.* Comparative Sol–Hydro (Solvo) thermal Synthesis of TiO_2 Nanocrystals // European Journal of Inorganic Chemistry. 2006. 11. P. 2229–2235.
https://doi.org/10.1002/ejic.200500855
19. *Wu M., Lin G., Chen D., Wang G., He D., Feng S., Xu R.* Solhydrothermal synthesis and hydrothermally structural evolution of nanocrystal titanium dioxide // Chemistry of Materials. 2002. 14. 5. P. 1974–1980.
https://doi.org/10.1021/cm0102739
20. *Wang C. C., Ying J. Y.* Sol–gel synthesis and hydrothermal processing of anatase and rutile titania nanocrystals // Chemistry of Materials. 1999. 11. P. 3113–3120.
https://doi.org/10.1021/cm990180f
21. *Castrejon-Sanchez V., Lopez R., Ramon-Gonzalez M., Enriquez-Perez A., Camacho-Lopez M., Villa-Sanchez G.* Annealing control on the anatase/rutile ratio of nanostructured titanium dioxide obtained by sol–gel // Crystals. 2018. **9**. 1. P. 22.
https://doi.org/10.3390/cryst9010022
22. *Bamne J., Sharma P.K., Haque F.Z.* Effect of solvent mixing and calcination temperature on the growth of TiO_2 nanoparticle prepared via sol–gel method // Materials Focus. 2018. **7**. 2. P. 232–241.
https://doi.org/10.1166/mat.2018.1502
23. *Luttrell T., Halpegamage S., Tao J., Kramer A., Sutter E., Batzill M.* Why is anatase a better photocatalyst than rutile? Model studies on epitaxial TiO_2 films // Scientific Reports. 2015. 4. 1. P. 4043. https://doi.org/10.1038/srep04043
24. *Di Paola A., Bellardita M., Palmisano L.* Brookite, the least known TiO_2 photocatalyst // Catalysts. 2013. **3**. 1. 36–73.
https://doi.org/10.3390/catal 3010036
25. *Qiu Y, Ouyang F, Zhu R.* A facile nonaqueous route for preparing mixed-phase TiO_2 with high activity in photocatalytic hydrogen generation // International Journal of Hydrogen Energy. 2017. 42. 16. 11364–11371.
https://doi.org/10.1016/j.ijhydene.2017.03.047
26. *Lei J., Li H., Zhang J., Anpo M.* Mixed-phase TiO_2 nanomaterials as efficient photocatalysts. In: Unlu H, Horing NJM, Dabowski J

(eds) Low-dimensional and nanostructured materials and devices // NanoScience and Technology. Springer. 2016.
https://doi.org/10.1007/978-3-319-25340-4_17

27. *Fischer K., Gawel A., Rosen D., Krause M., Abdul Latif A., Griebel J., Prager A., Schulze A.* Low-temperature synthesis of anatase/rutile/brookite TiO_2 nanoparticles on a polymer membrane for photocatalysis // Catalysts. 2017. **7**. 7. 209.
https://doi.org/10.3390/catal7070209
28. *Романовська Н. І., Гребенніков В. М., Шульженко О. В., Яремов П. С., Селищев О. В., Цан Д.Р.Т. (D.R.T. Zahn), Манорик П. А.* Вплив умов отримання наноструктур C,N,F-TiO_2 на їхню фотокаталітичну активність у процесі фотодеградації доксицикліну // Теоретична і експериментальна хімія. 2022. 58. 1. С. 35–41.
29. *Ohtani B., Prieto-Mahaney O.O., Li D., Abe R.* What is Degussa (Evonik) P25? Crystalline composition analysis, reconstruction from isolated pure particles and photocatalytic activity test // Journal of Photochemistry and Photobiology A: Chemistry. 2010. V. 216. Issues 2–3. P. 179–182.
30. *Mahshid S., Askari M., Sasani Ghamsari M., Afshar N., Lahuti S.* Mixed-phase TiO_2 nanoparticles preparation using sol–gel method // Journal of Alloys and Compounds. 2009. 478. (1–2). 586–589.
https://doi.org/10.1016/j.jallc om.2008.11.094
31. *Fresno F., Portela R., Suárez S., Coronado J. M.* Photocatalytic materials: recent achievements and near future trends // Journal of Material Chemistry A. 2014. 2. 9. P. 2863–2884.
https://doi.org/10.1039/C3TA13793G
32. *Ermokhina N. I., Nevinskiy V. A., Manorik P. A., Ilyin V. G., Shcherbatyuk M. M., Klymchyuk D. O., Puziy A. M.* Synthesis of large-pore mesoporous nanocrystalline TiO_2 microspheres // Materials Letters. 2012. 75. 68–70.
https://doi.org/10.1016/j.matlet.2012.01.133
33. *Ermokhina N. I., Nevinskiy V. A., Manorik P. A., Ilyin V. G., Novichenko V. N., Shcherbatiuk M. M., Klymchuk D. O., Tsyba M. M., Puziy A. M.* Synthesis and characterization of thermally stable large-pore mesoporous nanocrystallineanatase // Journal of Solid State Chemistry. 2013. 200. 90–98.
https://doi.org/10.1016/j.jssc.2012.12.034
34. *Stroyuk O. L., Ermokhina N. I., Korzhak G. V., Andryushina N. S., Shvalagin V. V., Kozytskiy A. V., Manoryk P. A., Barakov R. Y., Kuchmiy S. Y., Shcherbatyuk M. M., Sapsay V. I, Puziy A. M.* Photocatalytic and photoelectrochemical properties of hierarchical mesoporous TiO_2 microspheres produced using a crown template // Journal of Photochemistry and Photobiology A: Chemistry. 2017. 334. 26–35.
https://doi.org/10.1016/j.jphotochem.2016.10.039
35. *Stroyuk A. L., Ermokhina N. I., Korzhak A. V., Andryushina N. S., Kozytskiy A. V., Manorik P. A., Ilyin V. G., Puziy A. M., Sapsay V. I., Shcherbatyuk M. M.* Photocatalytic and photoelectrochemical characteristics of mesoporous titanium dioxide microspheres // Theoretical and Experimental Chemistry. 2015. 51. 3. 183–190.
https://doi.org/10.1007/s11237-015-9414-x
36. *Shvalagin V., Ermokhina N., Romanovska N., Barakov R., Manorik P., Sapsay V., Shcherbakov S., Poddubnaya O., Puziy A.* Mesoporous TiO_2 microspheres with improved efficiency for photooxidation of volatile organic compounds // Research Chemical Intermediates. 2019. 45. 8. 4133–4148.
https:// doi.org/10.1007/s11237-015-9414-x
37. *Ermokhina N. I., Shvalagin V. V., Romanovska N. I., Sydorova N. A., Manoryk P. A., Barakov R. Y., Shcherbatyuk M. M., Klymchuk D. O., Puziy A. M.* Photocatalytic activity of mesoporous titanium dioxide stabilized with lanthanum in the gas-phase oxidation of ethanol // Theoretical and Experimental Chemistry. 2018. 53. 6. 395–401.
https://doi.org/10.1007/s11237-018-9537-y

38. *Єрмохіна Н. І., Коржак Г. В., Романовська Н. І., Гребенніков В. М., Шульженко О. В., Климчук Д. О., Пузий А. М., Манорик П. А.* Фотокаталітична активність мезопористого TiO_2 (анатаз) у реакції виділення водню з водно-етанольної суміші // Український хімічний журнал. 2022. 88. 4. С. 94–112. Doi:10.33609/2708-129X.88.04.2022.94-112
39. *Раевская А. Е., Коржак А. В., Строюк А. Л., Кучмий С. Я.* Фотокаталитическое выделение водорода из водно-спиртовых сред с участием мезопористого TiO_2. // Теоретическая и экспериментальная химия. 2009. 45. 6. С. 331–335.
40. *Cano-Casanova L., Amoros-Perez A., Lillo-Rodenas M., Roman-Martinez M.* Effect of the preparation method (sol–gel or hydrothermal) and conditions on the TiO_2 properties and activity for propene oxidation // Materials. 2018 (Basel). 11. 11. 2227. https://doi.org/10.3390/ma11112227
41. *Kaplan R., Erjavec B., Dražić G., Grdadolnik J., Pintar A.* Simple synthesis of anatase/rutile/brookite TiO_2 nanocomposite with superior mineralization potential for photocatalytic degradation of water pollutants // Applied Catalysis B: Environmental. 2016. 181. 465–474. https://doi.org/10.1016/j.apcatb.2015.08.027
42. *Korzhak A. V., Ermokhina N. I., Stroyuk A. L., Bukhtiyarov V. K., Raevskaya A. E., Litvin V. I., Kuchmiy S. Y., Ilyin V. G., Manorik P. A.* Photocatalytic hydrogen evolution over mesoporous TiO_2/metal nanocomposites // Journal of Photochemistry and Photobiology A: Chemistry. 2008. 198. 2. P. 126–134. http://dx.doi.org/10.1016/j.jphotochem.2008.02.026
43. *Ermokhina N. I., Shvalagin V. V., Romanovska N. I., Manoryk P. A., Barakov R. Yu., Kompanets M. O.,·Sapsay V. I., Klymchuk D. O., Puziy A. M.* Synthesis and characterization of different binary and ternary phasemixtures of mesoporous nanocrystalline titanium dioxide // SN Applied Sciences. 2021. 3. 491. https://doi.org/10.1007/s42452-021-04474-y
44. *Tobaldi D. M., Lajaunie L., Rozman N., Caetano APF., Seabra M.P., Sever Škapin A., Arenal R., Labrincha J. A.* Impact of the absolute rutile fraction on TiO_2 visible-light absorption and visible-light-promoted photocatalytic activity // Journal of Photochemistry and Photobiology A: Chemistry. 2019. 382. 111940. https://doi.org/10.1016/j.jphotochem.2019.111940

REFERENCES

1. Kryukov A. I., Stroyuk A. L., Kuchmiy S. YA., Pokhodenko V. D. Nanofotokataliz. Kyiv: Akademperiodika. 2013. 618. (in Russian).
2. Schneider J., Bahnemann D., Ye J., Puma, G. Li., Dionysiou D. D. Photocatalysis: fundamentals and perspectives. *Royal Society of Chemistry*. *Cambridge*. 2016. https://doi.org/10.1039/9781782622338
3. Wang Y., Sun C., Zhao X., Cui B., Zeng Z., Wang A., Liu G., Cui H. The application of nano-TiO_2 photo semiconductors in agriculture. *Nanoscale Research Letters*. 2016. **11**(1): 529. http://dx.doi.org/10.1186/s11671-016-1721-1
4. Kumar N., Chauhan N.S., Mittal A., Sharma S. TiO_2 and its composites as promising biomaterials: a review. *BioMetals*. 2018. **31**(2): 147–159. https://doi.org/10.1007/s10534-018-0078-6
5. Noman M. T., Ashraf M. A., Ali A. Synthesis and applications of nano-TiO_2: a review. *Environmental Science and Pollution Research.* 2019. **26**(4): 3262–3291. https://doi.org/10.1007/s11356-018-3884-z
6. Humayun M., Raziq F., Khan A., Luo W. Modification strategies of TiO_2 for potential applications in photocatalysis: a critical review. *Green Chemistry Letters and Reviews*. 2018. **11**(2): 86–102. https://doi.org/10.1080/17518253.2018.1440324
7. Paul K. K., Giri P. K. Shape tailored TiO_2 nano-

structures and their hybrids for advanced energy and environmental applications: a review. *Journal of Nanoscience and Nanotechnology*. 2018. **19**(1): 307–331. https://doi.org/10.1166/jnn.2019.15778

8. Dionysiou D. D., Puma G. Li., Ye J., Schneider J., Bahnemann D. Photocatalysis: Applications. *Royal Society of Chemistry. Cambridge*. 2016. 394. https://doi.org/10.1039/9781782627104
9. Anpo M., Kamat P. V. Environmentally benign photocatalysts. *Springer.* New York. 2010. https://doi.org/10.1007/978-0-387-48444-0
10. Laura Cano-Casanova, Ana Amorós-Pérez, Maria Angeles Lillo-Ródenas and María del Carmen Román-Martínez. Effect of the preparation method (sol–gel or hydrothermal) and conditions on the TiO_2 properties and activity for propane oxidation. *Materials* (Basel). 2018. **11**(11): 2227. https://doi.org/10.3390/ma11112227
11. Verma R, Gangwar J, Srivastava A.K. Multiphase TiO_2 nanostructures: a review of efficient synthesis, growth mechanism, probing capabilities, and applications in bio-safety and health. *RSC Advances*. 2017. **7**: 44199–44224. https://doi.org/10.1039/C7RA06925A
12. Bagheri S, Julkapli NM. Mixed-phase TiO_2 photocatalysis: correlation between phase composition and photodecomposition of water pollutants. *Reviews Inorganic Chemistry*. 2017. **37**(1): 11–28. https://doi.org/10.1515/revic-2016-0001
13. Kumar A. Different methods used for the synthesis of TiO_2 based nanomaterials: a review. *American Journal of Nano Research and Application*. 2018. **6**(1): 1. https://doi.org/10.11648/j.nano.20180601.11
14. Shayegan Z., Lee C-S., Haghighat F. TiO_2 photocatalyst for removal of volatile organic compounds in gas phase: a review. *Chemical Engineering Journal*. 2018. **334**: 2408–2439. https://doi.org/10.1016/j.cej.2017.09.153
15. Paul KK, Giri PK. Shape tailored TiO_2 nanostructures and their hybrids for advanced energy and environmental applications: a review. *Journal Nanoscience Nanotechnology*. 2018. **19**(1): 307–331. https://doi.org/10.1166/jnn.2019.15778
16. Jiang, Z., Xu, X., Ma, Y. et al. Filling metal–organic framework mesopores with TiO_2 for CO_2 photoreduction. *Nature*. 2020. **586**: 549–554. https://doi.org/10.1038/s41586-020-2738-2
17. Jing Ma, Yang Tang, Gui Lu, Yu Wang, Wenke Niu, Dong Fu, Kai Zhang, Detlef W. Bahnemann, and Jia Hong Pan. Incorporating Mesoporous Anatase TiO_2 Spheres to Conductive Carbon Black Filled PVDF Membrane for Self-Cleaning Photo (electro) catalytic Filtration. *Journal of Physical Chemistry* C. 2023. **127**(17): 7998–8005. https://doi.org/10.1021/acs.jpcc.3c01346
18. Yang X., Konishi H., Xu H., Wu M. Comparative Sol–Hydro (Solvo) thermal Synthesis of TiO_2 Nanocrystals. *European Journal of Inorganic Chemistry*. 2006. **11**: 2229–2235. https://doi.org/10.1002/ejic.200500855
19. Wu M., Lin G., Chen D., Wang G., He D., Feng S., Xu R. Solhydrothermal synthesis and hydrothermally structural evolution of nanocrystal titanium dioxide. *Chemistry of Materials*. 2002. **14**(5): 1974–1980. https://doi.org/10.1021/cm0102739
20. Wang C. C., Ying J. Y. Sol–gel synthesis and hydrothermal processing of anatase and rutile Titania nanocrystals. *Chemistry of Materials*. 1999. **11**(11): 3113–3120. https://doi.org/10.1021/cm990180f
21. Castrejon-Sanchez V., Lopez R., Ramon-Gonzalez M., Enriquez-Perez A., Camacho-Lopez M., Villa-Sanchez G. Annealing control on the anatase/rutile ratio of nanostructured titanium dioxide obtained by sol–gel. *Crystals*. 2018. **9**(1): 22. https://doi.org/10.3390/cryst9010022
22. Bamne J., Sharma P.K., Haque F.Z. Effect of solvent mixing and calcination temperature on the growth of TiO_2 nanoparticle prepared

via sol–gel method. *Materials Focus*. 2018. **7**(2): 232–241. https://doi.org/10.1166/mat.2018.1502

23. Luttrell T., Halpegamage S., Tao J., Kramer A., Sutter E., Batzill M. Why is anatase a better photocatalyst than rutile? Model studies on epitaxial TiO_2 films. *Scientific Reports*. 2015. **4**(1): 4043. https://doi.org/10.1038/srep04043
24. Di Paola A., Bellardita M., Palmisano L. Brookite, the least known TiO_2 photocatalyst. *Catalysts*. 2013. **3**(1): 36–73. https://doi.org/10.3390/catal 3010036
25. Qiu Y, Ouyang F, Zhu R. A facile nonaqueous route for preparing mixed-phase TiO_2 with high activity in photocatalytic hydrogen generation. *International Journal of Hydrogen Energy*. 2017. **42** (16): 11364–11371. https://doi.org/10.1016/j.ijhydene.2017.03.047
26. Lei J., Li H., Zhang J., Anpo M. Mixed-phase TiO_2 nanomaterials as efficient photocatalysts. In: Unlu H, Horing NJM, Dabowski J (eds) Low-dimensional and nanostructured materials and devices. NanoScience and Technology. *Springer*. 2016. https://doi.org/10.1007/978-3-319-25340-4_17
27. Fischer K., Gawel A., Rosen D., Krause M., Abdul Latif A., Griebel J., Prager A., Schulze A. Low-temperature synthesis of anatase/rutile/brookite TiO_2 nanoparticles on a polymer membrane for photocatalysis. *Catalysts*. 2017. **7**(7): 209. https://doi.org/10.3390/catal7070209
28. Romanovs'ka N. I., Hrebennikov V. M., Shul'zhenko O. V., Yaremov P. S., Selishchev O. V., Tsan D.R.T. (D.R.T.Zahn), Manoryk P. A. Vplyv umov otrymannya nanostruktur C,N,F-TiO_2 na yikhnyu fotokatalitychnu aktyvnist' u protsesi fotodehradatsiyi doksytsyklinu. *Teoretychna ta eksperymental'na khimiya*. 2022. **58**(1): 35–41. (In Ukrainian).
29. Ohtani B., Prieto-Mahaney O.O., Li D., Abe R. What is Degussa (Evonik) P25? Crystalline composition analysis, reconstruction from isolated pure particles and photocatalytic activity test. Journal of Photochemistry and Photobiology A: *Chemistry*. 2010. **216**(2–3): 179–182.
30. Mahshid S., Askari M., Sasani Ghamsari M., Afshar N., Lahuti S. Mixed-phase TiO_2 nanoparticles preparation using sol–gel method. *Journal of Alloys and Compounds*. 2009. **478**(1–2): 586–589. https://doi.org/10.1016/j.jallc om.2008.11.094
31. Fresno F., Portela R., Suárez S., Coronado J. M. Photocatalytic materials: recent achievements and near future trends. *Journal of Material Chemistry* A. 2014. **2**(9): 2863–2884. https://doi.org/10.1039/C3TA13793G
32. Ermokhina N. I., Nevinskiy V. A., Manorik P. A., Ilyin V. G., Shcherbatyuk M. M., Klymchyuk D. O., Puziy A. M. Synthesis of large-pore mesoporous nanocrystalline TiO_2 microspheres. *Materials Letters*. 2012. **75**: 68–70. https://doi.org/10.1016/j.matlet.2012.01.133
33. Ermokhina N. I., Nevinskiy V. A., Manorik P. A., Ilyin V. G., Novichenko V. N., Shcherbatiuk M. M., Klymchuk D. O., Tsyba M. M., Puziy A. M. Synthesis and characterization of thermally stable large-pore mesoporous nanocrystalline-anatase. *Journal of Solid State Chemistry*. 2013. **200**: 90–98. https://doi.org/10.1016/j.jssc.2012.12.034
34. Stroyuk O. L., Ermokhina N. I., Korzhak G. V., Andryushina N. S., Shvalagin V. V., Kozytskiy A. V., Manoryk P. A., Barakov R. Y., Kuchmiy S. Y., Shcherbatyuk M. M., Sapsay V. I, Puziy A. M. Photocatalytic and photoelectrochemical properties of hierarchical mesoporous TiO_2 microspheres produced using a crown template. *Journal of Photochemistry and Photobiology* A: *Chemistry*. 2017. **334**: 26–35. https://doi.org/10.1016/j.jphotochem.2016.10.039
35. Stroyuk A. L., Ermokhina N. I., Korzhak A. V., Andryushina N. S., Kozytskiy A. V., Manorik P. A., Ilyin V. G., Puziy A. M., Sapsay V. I., Shcherbatyuk M. M. Photocatalytic and photoelectrochemical characteristics of mesoporous

titanium dioxide microspheres. *Theoretical and Experimental Chemistry*. 2015. **51**(3): 183–190.
https://doi.org/10.1007/s11237-015-9414-x

36. Shvalagin V., Ermokhina N., Romanovska N., Barakov R., Manorik P., Sapsay V., Shcherbakov S., Poddubnaya O., Puziy A. Mesoporous TiO_2 microspheres with improved efficiency for photooxidation of volatile organic compounds. *Research Chemical Intermediates*. 2019. **45**(8): 4133–4148.
https:// doi.org/10.1007/s11237-015-9414-x
37. Ermokhina N. I., Shvalagin V. V., Romanovska N. I., Sydorova N. A., Manoryk P. A., Barakov R. Y., Shcherbatyuk M. M., Klymchuk D. O., Puziy A. M. Photocatalytic activity of mesoporous titanium dioxide stabilized with lanthanum in the gas-phase oxidation of ethanol. *Theoretical and Experimental Chemistry*. 2018. **53**(6): 395–401.
https://doi.org/10.1007/s11237-018-9537-y
38. Yermokhina N. I., Korzhak G. V., Romanovskaya N. I., Grebennikov V. M., Shul'zhenko O. V., Klimchuk D. O., Puzyy A. M., Manorik P. A. Fotokataliticheskaya aktivnost' mezoporistogo TiO_2 (anataz) v reaktsii vydeleniya vodoroda iz vodno-etanol'noy smesi. *Ukrainskiy khimicheskiy zhurnal*. 2022. **88**(4): 94–112. (In Ukrainian).
Doi:10.33609/2708-129X.88.04.2022.94-112
39. Rayevs'ka O. YE., Korzhak O. V., Stroyuk O. L., Kuchmiy S. YA. Fotokatalitychne vydilennya vodnyu z vodno-spyrtovykh seredovyshch za uchastyu mezoporystoho TiO_2. *Teoretychna ta eksperymental'na khimiya*. 2009. **45**(6): 331–335. (in Russian).
40. Cano-Casanova L., Amoros-Perez A., Lillo-Rodenas M., Roman-Martinez M. Effect of the preparation method (sol–gel or hydrothermal) and conditions on the TiO_2 properties and activity for propene oxidation. *Materials*. 2018 (Basel). **11**(11): 2227.
https://doi.org/10.3390/ma11112227
41. Kaplan R., Erjavec B., Dražić G., Grdadolnik J., Pintar A. Simple synthesis of anatase/rutile/brookite TiO_2 nanocomposite with superior mineralization potential for photocatalytic degradation of water pollutants. *Applied Catalysis B: Environmental*. 2016. **181**: 465–474.
https://doi.org/10.1016/j.apcatb.2015.08.027
42. Korzhak A. V., Ermokhina N. I., Stroyuk A. L., Bukhtiyarov V. K., Raevskaya A. E., Litvin V. I., Kuchmiy S. Y., Ilyin V. G., Manorik P. A. Photocatalytic hydrogen evolution over mesoporous TiO_2/metal nanocomposites. *Journal of Photochemistry and Photobiology A*: *Chemistry*. 2008. **198**(2): 126–134.
http://dx.doi.org/10.1016/j.jphotochem.2008.02.026
43. Ermokhina N. I., Shvalagin V. V., Romanovska N. I., Manoryk P. A., Barakov R. Yu., Kompanets M. O.,·Sapsay V. I., Klymchuk D. O., Puziy A. M. Synthesis and characterization of different binary and ternary phasemixtures of mesoporous nanocrystalline titanium dioxide. *SN Applied Sciences*. 2021. **3**: 491.
https://doi.org/10.1007/s42452-021-04474-y
44. Tobaldi D. M., Lajaunie L., Rozman N., Caetano APF., Seabra M.P., Sever Škapin A., Arenal R., Labrincha J. A. Impact of the absolute rutile fraction on TiO_2 visible-light absorption and visible-light-promoted photocatalytic activity. *Journal of Photochemistry and Photobiology A: Chemistry*. 2019. **382**: 111940.
https://doi.org/10.1016/j.jphotochem.2019.111940

Стаття надійшла 15.12.2023.